12. Light Flash Observations

Experiment MA-106

T. F. Budinger,[a†] C. A. Tobias,[a] R. H. Huesman,[a] F. T. Upham,[a] T. F. Wieskamp,[b] J.-U. Schott,[c] and E. Schopper [c]

ABSTRACT

There were 82 visual events reported by two dark-adapted crewmembers during a 90-minute orbit at an altitude of 225 km. Silver chloride crystal events for that orbit totaled 69 stopping protons and alpha particles per square centimeter and 304 heavy ions with linear energy transfer of 150 MeV cm^2/g or greater. Frequency of visual observations near the geomagnetic poles corresponds to calculated abundances of ions with linear energy transfer greater than 5 keV/μm in tissue. Alpha particles from nonelastic nuclear collisions of fast protons on carbon, nitrogen, and oxygen in the retina or the abundance of stopping protons can explain the low frequency of events in the South Atlantic Anomaly for this mission compared to the high frequency during Skylab 4 at a 443-km altitude.

INTRODUCTION

During the last six Apollo missions and on a few occasions during Skylab, the crews made both scheduled and unscheduled observations of the frequency and character of tiny starlike, brief flashes of white light or pencil-thin streaks of light (refs. 12-1 to 12-6). These observations can be summarized as follows. After approximately 17 minutes of dark adaptation, tiny dots and thin streaks of white light were seen at frequencies of approximately 3 events/min by crewmembers when on translunar or transearth coast or over the polar part of Skylab orbits. When near the South Atlantic Anomaly (SAA), where the proton flux is more than 1000 times greater than in other parts of the orbit, the frequency increased to approximately 9 events/min for Skylab altitudes of 443 km (ref. 12-6). Examples of the type of phenomena seen are shown in figure 12-1, which is based on descriptions by Apollo and Skylab crews as well as laboratory experiments with accelerated charged particles.

Astronaut Edwin E. Aldrin, Jr., first reported these visual phenomena. They were predicted in 1952 by C. A. Tobias (ref. 12-7), who hypothesized that astronauts were likely to see flashes of light from cosmic particles when they were outside the shielding provided by the Earth's magnetic field. The site of action of these particles, and whether cosmic particles actually caused the light flash phenomenon, were subjects of conjecture in 1970 when this phenomenon was first reported. Many known causes for luminous phosphenes exist, including ionizing radiation, mechanical pressure, electrical currents, magnetic fields, stimulation of the cerebral cortex, and pathological conditions of the central nervous system. For example, flashes can be seen during stages of retinal detachment, and the retina is sensitive to externally applied currents as small as 0.3 mA. In 1970, these phenomena were believed to be caused by ionizing heavy nuclei such as carbon,

[a]Lawrence Berkeley Laboratory, University of California at Berkeley.

[b]Lawrence Livermore Laboratory.

[c]University of Frankfurt.

[†]Principal Investigator.

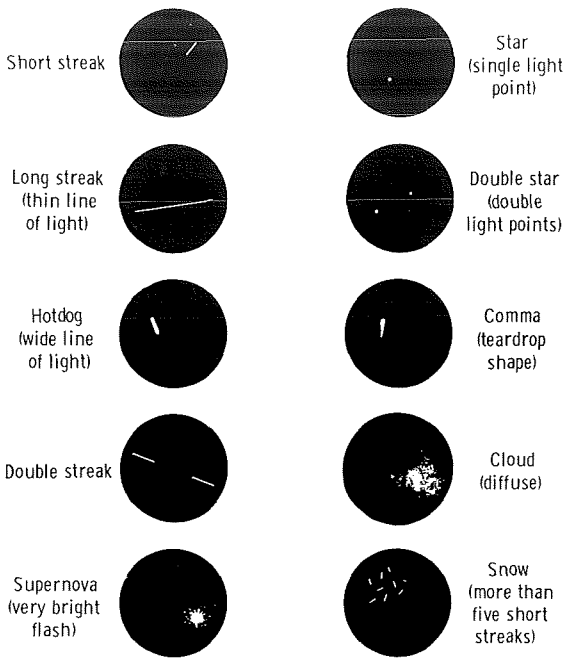

FIGURE 12-1.—Reproduction of visual events noted in space and in cyclotron experiments.

nitrogen, and oxygen, which traverse the spacecraft and the body at frequencies of 1 to 2 nuclei/min • cm^2 when outside the Earth's magnetic shielding. Of continuing controversy is the conjecture that the major mechanism for these visual phenomena is Cerenkov radiation (refs. 12-8 to 12-11).

In 1970, a series of experiments was conducted to determine whether carbon, nitrogen, and oxygen of approximately 300 MeV/amu and other ions with equivalent ionizing characteristics could cause qualitatively the same phenomena seen by astronauts. Ionizing particles with linear energy transfer (LET) of approximately 10 keV/μm or greater caused similar phenomena in a series of experiments using neutrons of 630 MeV energy, neutrons of approximately 8 MeV energy, helium ions from the 467-cm (184 in.) cyclotron at 230 MeV/nucleon, and nitrogen ions accelerated to approximately 260 MeV/nucleon at the Bevatron (refs. 12-12 to 12-15). These experiments demonstrated that ionization or electronic excitation from cosmic particles could adequately account for the light flash phenomenon. Cerenkov light is produced by particles at velocities greater than those used in the experiments just described; therefore, it was concluded that, whereas Cerenkov radiation might cause similar phenomena, it was not the predominant mechanism. It is still unclear as to the exact mechanism whereby the retina is stimulated by ionizing particles at velocities below those necessary for emission of Cerenkov light. Experiments in which nitrogen ions were stopped in nine positions in the cerebral cortex have shown that the brain and the optic nerve are not stimulated by ions (ref. 12-15). The mechanisms by which cosmic particles can produce visual sensations are electronic excitation resulting in near-ultraviolet (UV) radiation in the vicinity of the retina, ionization by the primary cosmic particle along the track through the retina, local ionization by the products of a nonelastic collision between a high-velocity proton and carbon, nitrogen, or oxygen, or a shock wave phenomenon from energetic charged particles passing through the tissue matrix.

The purpose of this experiment was to ascertain quantitatively the frequency, character, latitudinal dependence, and identity of cosmic particles that cause the light flash phenomenon. The ultimate objective was the assessment of radiation hazards of long-term Earth-orbiting and interplanetary missions. The special features of this experiment included measurement of the characteristics of the cosmic-particle environment in the vicinity of the eye, measurement of dark adaptation, and continuous onboard accumulation of the light flash observations from astronauts and particle detectors throughout one complete orbit.

EQUIPMENT

The equipment for the experiment consisted of two dark adaptation masks, two pushbuttons, two cosmic-particle detector boxes, and a control and power unit that housed a data tape. The masks and pushbuttons were manned by two crewmembers, and the control and power unit was controlled by the third crewmember, who monitored the experiment (figs. 12-2 and 12-3).

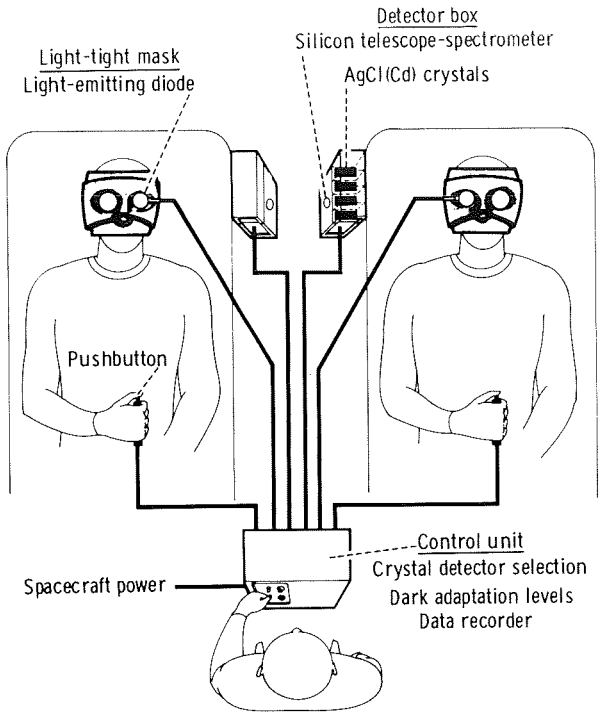

FIGURE 12-2.—Experiment layout.

Dark Adaptation Masks

Each dark adaptation mask was made of Lexan plastic approximately 2 mm thick and was fitted with a light-emitting diode (LED) behind a pinhole aperture approximately 2 cm from one eye. The masks, held to the head by straps, were fabricated from molds of each crewmember's head. Plaster of paris head casts were made from these molds. The Lexan masks were then made by pressing near-molten Lexan over these head casts. The resulting mask was nearly light tight. To ensure a perfect light-tight fit, a foam rubber insert was used and each mask was then custom fitted to each crewmember.

The effective brightness of the LED was controlled by the duration of a constant voltage. The duration ranged from 5 microseconds to 1.7 milliseconds in six different levels and produced the expected response on normal subjects in terms of the rapidity with which each level of dark adaptation was reached. Level 5 was reached approximately 15 minutes after commencement of dark adaptation.

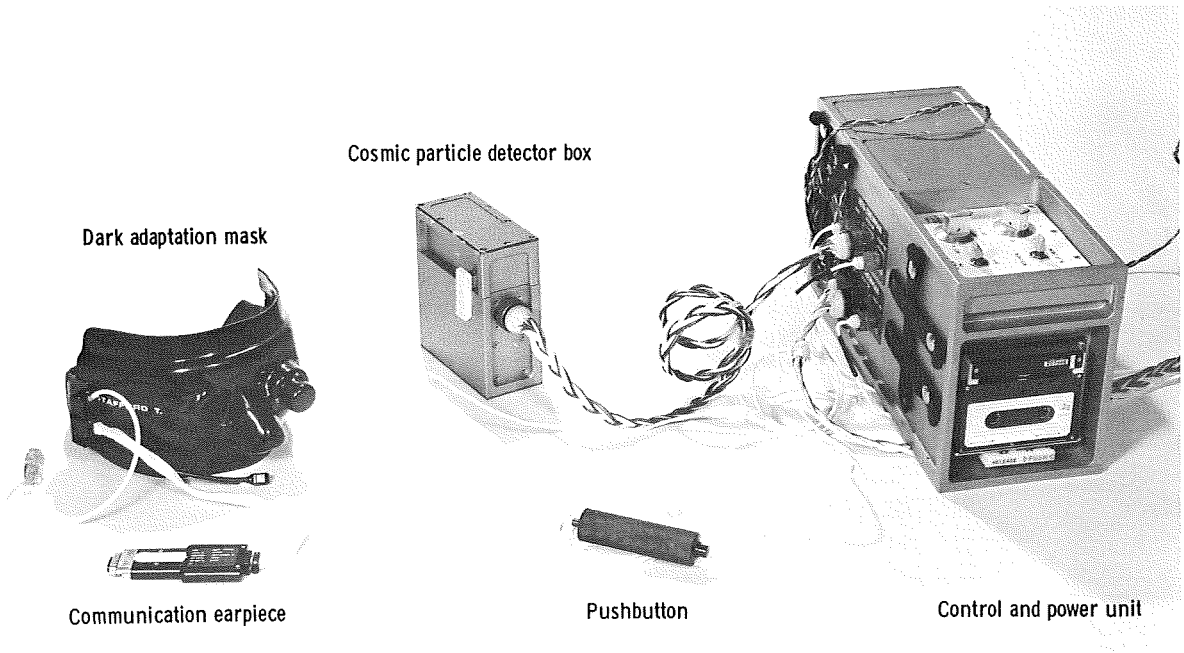

FIGURE 12-3.—Experiment hardware.

Detector Boxes

Each of the two detector units contained silver chloride (cadmium doped) (AgCl(Cd)) crystals and a silicon solid-state telescope-spectrometer. The location of the detector boxes in the command module is shown in figure 12-4. Each detector box was composed of two units. The first unit (4.1 by 5.5 by 12.7 cm) was an aluminum housing in which there were four compartments (each 1.84 by 3.5 by 2.75 cm) for AgCl(Cd) crystals and small lights. The AgCl(Cd) crystals were 1- by 2-cm wafers 0.03 cm thick. Two crystals were placed in each compartment on either side of two white 6-V lights, which were filtered to give predominantly yellow light by using yellow plastic sheets (Kapton, 0.06 cm thick) between the lights and crystals.

The AgCl(Cd) crystals are nuclear particle detectors developed in Germany (ref. 12-16). They are similar to nuclear emulsions but have a unique property that allows evaluation of the time during which a particle traverses the detector. A nuclear particle passing through the crystal leaves a latent track of dislocated electrons and displaced silver or cadmium atoms. Within a few minutes, the migration of electrons and atoms returns the crystal to its original condition. However, if the crystal is exposed to visual spectrum photons, the latent track is fixed or stabilized. Hours or weeks later, if the crystal is exposed to UV light, the stabilized but still invisible tracks are developed, leaving a permanent record of the nuclear particle track. The distribution of residual silver around the track is related to the charge and velocity of the ion as well as to the intensity and spectrum of

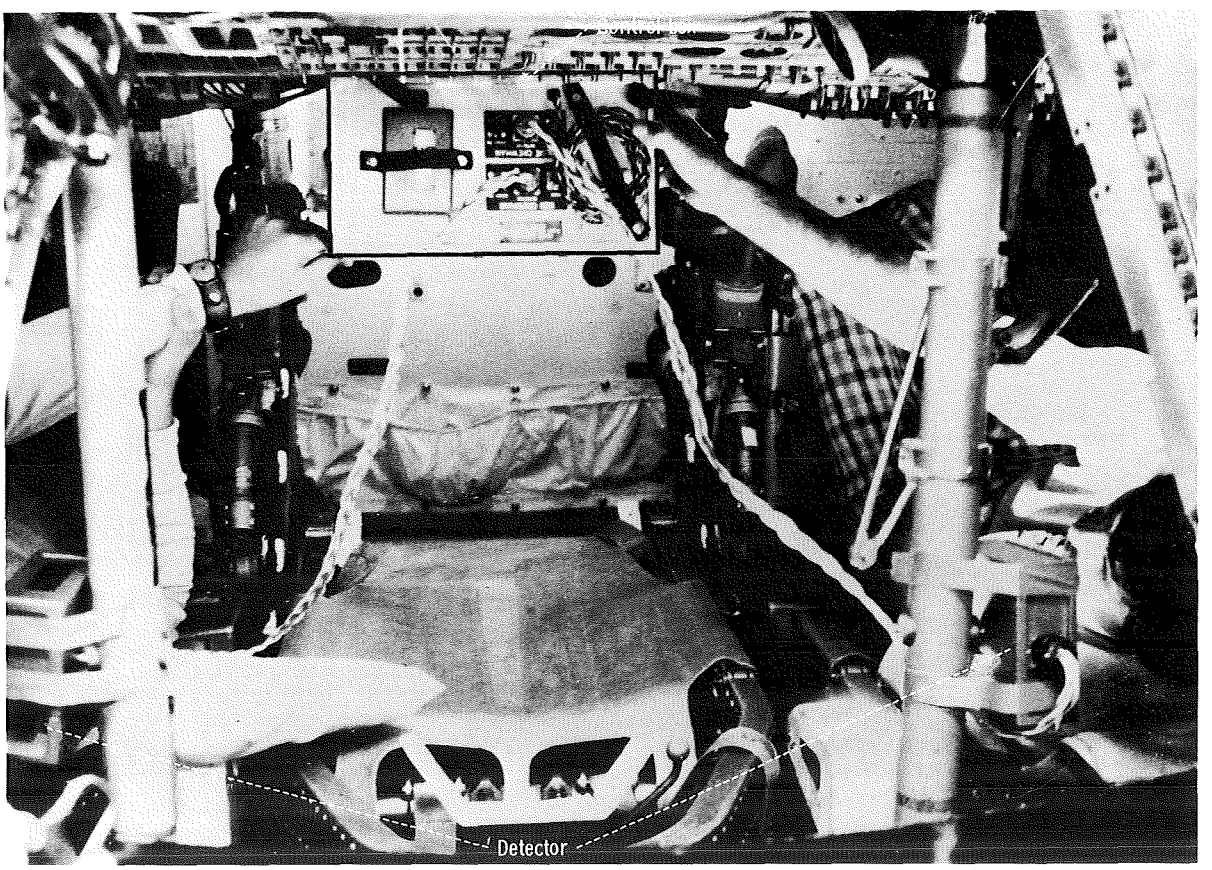

FIGURE 12-4.—Location of equipment in spacecraft.

near-UV light used to develop the stabilized tracks. The time period between implantation of a latent track and fading is a few minutes, but the period between the time a stabilized track is made and fading is more than 1 week. Crystals were loaded into each of four compartments so that the particle environment could be measured in the four sectors of the orbit corresponding to the northern latitudes, the equatorial latitudes, the SAA, and the remaining minutes of the orbit over the Pacific Ocean.

The second unit (4.3 by 9.6 by 12.7 cm) of each detector box housed the electronic detector, which consisted of two sets of silicon solid-state wafers. Each set consisted of two individual wafers 1.7 cm in diameter and 0.03 cm thick. On each wafer were four active strips, each 3 mm wide, separated by 0.5 mm. The telescope was made by rotating one wafer 90° from the other. This set of two wafers gave 16 possible combinations (4 by 4) for particle position. The second set of two wafers was placed 1.5 cm from the first set, and a 0.5-cm-thick copper energy degrader was placed between the sets. This arrangement allowed measurement of the trajectory and energy loss of particles passing through the telescope. The threshold for the device is 100 MeV cm^2/g.

Pushbuttons

Events noted by astronauts were recorded on digital tape by means of a handheld pushbutton switch.

Control and Power Unit

The control and power unit consisted of power distribution, logic circuits, and a digital cassette tape recorder that received 16-bit word groups from the observer pushbuttons and the silicon detectors. Word groups from the silicon detectors contained information on the trajectory and energy loss of particles that passed through the silicon detector. Elapsed time and detector selector switch position information were also recorded.

EXPERIMENT PROTOCOL

Two revolutions were devoted to this experiment. During revolution 110, the silicon telescope-spectrometer was deployed for measurement of the trajectory, atomic charge Z, and velocity of cosmic particles with a stopping power of 10 keV/μm or greater. During revolution 111, the Apollo commander and the command module pilot made continuous observations of visual sensations while dark adapted. The docking module pilot operated the experiment control unit, which received data from the silicon detectors as well as from AgCl(Cd) crystals that were used to register particle tracks in four sectors of the orbit corresponding to northern latitudes, equatorial latitudes, the SAA, and southern latitudes.

The experiment commenced with the detector-alone orbit according to the Flight Plan at approximately 13:40 UT on July 22, 1975. The detector-manned orbit, revolution 111, began according to the Flight Plan at approximately 14:45 UT, at which time the spacecraft was maneuvering to proper attitude because the attitude for revolution 110 was not optimum. Approximately 10 minutes later, the observing crewmembers had reached dark adaptation. The first light flash was reported at 15:00 UT at latitude 49° N when the spacecraft was approaching the northernmost point of the orbit. At each event, a pushbutton signal from the observing astronaut was recorded on the digital tape and the verbal description was recorded on the onboard tape recorder. The docking module pilot switched the lighting for the AgCl(Cd) crystal compartments according to the Flight Plan at 17, 29, and 54 minutes after commencement of revolution 111. The experiment was terminated at 16:50 UT. In accordance with the Flight Plan, the digital tapes, voice tapes, detector boxes, and masks were returned to the experimenters. The digital tapes were transported to the Lawrence Berkeley Laboratory for analysis, and the AgCl(Cd) crystals were transported to the University of Frankfurt.

PROCEDURES FOR DATA REDUCTION

Observed Events

Descriptions of the events observed by the crewmembers were recorded on the onboard voice recorder. The tapes were transcribed, and each event was related to the orbital position of the spacecraft. Events from the silicon detectors and pushbuttons and the status of the control unit were read from the digital tape by a specially constructed microprocessor. The pushbutton events and time marks were related to the verbal reports. The energy and trajectory information was inadequate because of a paucity of recorded events.

The AgCl(Cd) crystals were transported to the University of Frankfurt, where they had been produced and calibrated. These crystals were analyzed for the abundance of tracks that are related to protons, alpha particles, or heavier ions.

Calculations of Expected Particle Dose

The characteristics of the cosmic-particle environment inside the spacecraft were determined by converting the spectrum and abundance of particles outside the spacecraft to the number of particles with various LET values and residual ranges, using shielding data for 512 sectors of solid angle around the spacecraft. The shielding data of equivalent thickness of aluminum were supplied by the NASA Lyndon B. Johnson Space Center. Spacecraft position and orientation were obtained from mission ephemeris data supplied after the flight. Cosmic-ray abundances for free space for $Z > 3$ were obtained from Webber et al. (ref. 12-17), and the abundances for hydrogen and helium were obtained from Smith et al. (ref. 12-18). The spectra were assumed to be the same as those for carbon and oxygen, which were obtained from Juliusson (ref. 12-19). For trapped protons, the model environment AP7 of Lavine and Vette (ref. 12-20) was used.

These free-space abundances were converted to the abundance outside the spacecraft at a 225-km altitude using the spacecraft orbit parameters of B[1] and L[2] data obtained from the 99-term field of Hendricks and Cain (ref. 12-21) extrapolated to 1975. Vertical rigidity cutoffs for cosmic particles at an altitude of 20 km were obtained from Shea and Smart (ref. 12-22). Translation to orbit altitudes (ref. 12-23) and nonvertical directions was performed (ref. 12-24).

The energy-range relationship was derived from an empirical formula that gives range R as a function of kinetic energy:

$$R = \frac{\alpha A}{Z^2}\left(\frac{E}{A}\right)^{\beta} \qquad (12\text{-}1)$$

where A is the atomic number, Z is the charge, and E is the energy in MeV/amu.

For passage of ions through the spacecraft, aluminum shielding is assumed. Thus, the constants are $\alpha = 2.811 \times 10^{-3}$ and $\beta = 1.775$. The stopping power S is given as

$$S = \frac{Z^2}{\alpha\beta}\left(\frac{E}{A}\right)^{1-\beta} \qquad (12\text{-}2)$$

Energy transfer in the eye is calculated using equation (12-2) and $\alpha = 1.88 \times 10^{-3}$ and $\beta = 1.802$, corresponding to the passage of ions through water.

RESULTS

Visual Observations

The distribution of visual events reported by astronauts is shown along the track line in figure 12-5. Histograms depicting the frequency of events in time and with respect to latitude are shown in figure 12-6. Because the spacecraft

[1] Geomagnetic field strength.

[2] Distance from the center of the Earth in Earth radii.

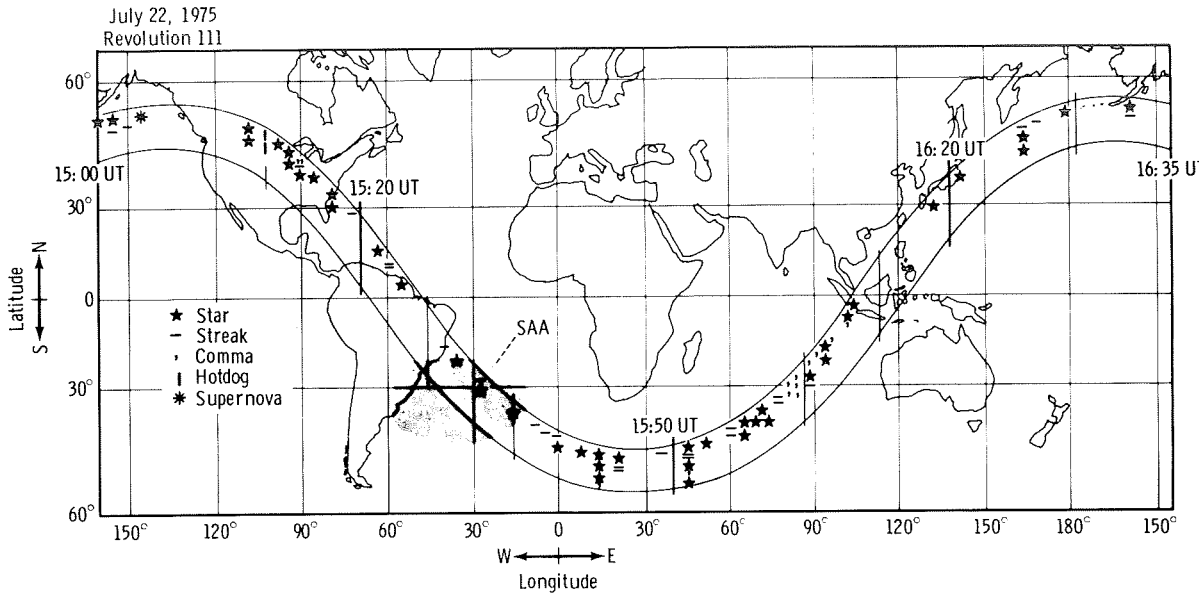

FIGURE 12-5.—Orbit track and distribution of reported events.

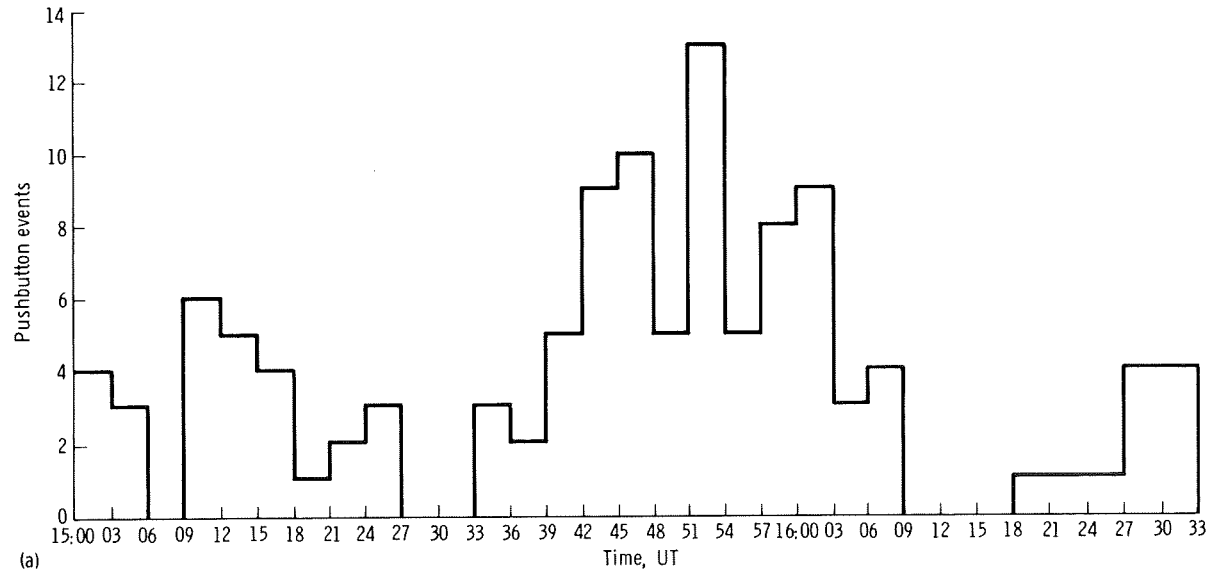

FIGURE 12-6.—Histograms of pushbutton events by time and latitude. Except for a few cases, pushbutton events agree with verbal reports. (a) Intervals of 3 minutes. (b) Intervals of 5° latitude. (c) Intervals of 5° latitude normalized by time intervals.

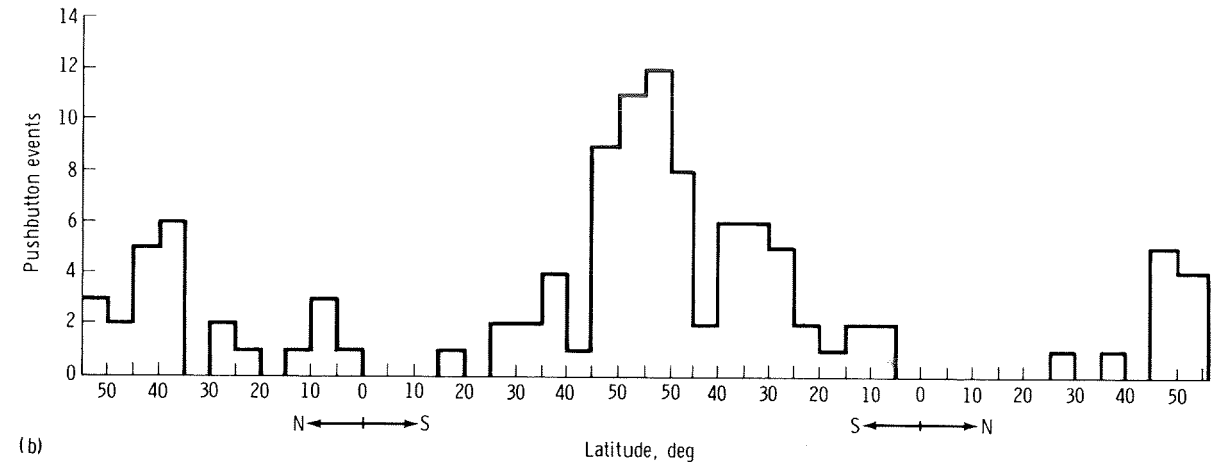

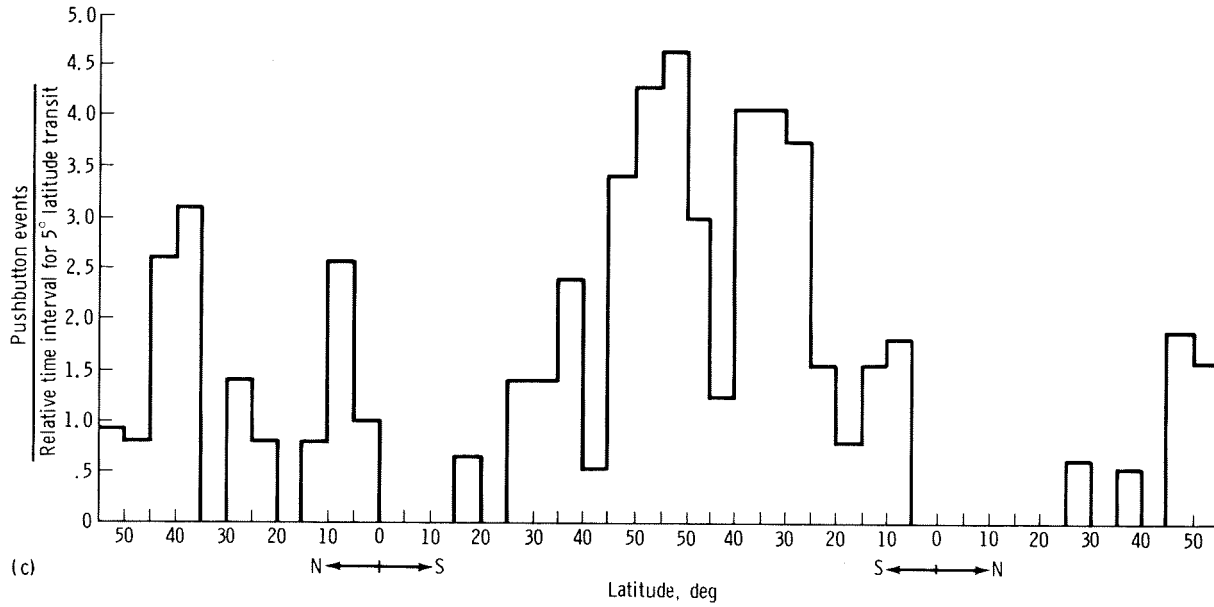

FIGURE 12-6.—Concluded.

TABLE 12-I.—Summary of Events

Track sector	*Stars (a)*	*Streaks (b)*	*Commas*	*Total*
Northernmost point of orbit to Florida	12	6	2	20
Florida to Brazil	2	3	0	5
SAA	2	1	0	3
SAA to completion of orbit	27	16	11	54

[a]Includes events expressed as supernovas in figure 12-1.
[b]Includes events expressed as hotdogs in figure 12-1.

TABLE 12-II.—Visual Flux and Particle Flux From AgCl (Cd) Detectors

UT (July 22, 1975), hr:min	*Lat.*	*Long.*	*Visual events*		*Stopping protons and alpha particles*		*Heavy ions, LET ≥ 15 keV/μm*[a]	
			No. reported	*No./hr*	*Events, cm^{-2} $sector^{-1}$*	*Flux, cm^{-2} hr^{-1}*	*Events, cm^{-2} $sector^{-1}$*	*Flux, cm^{-2} hr^{-1}*
14:56	43° N	179° E	20	71	14.0 ± 1.4	49	70.0 ± 4.8	250
15:13	38° N	90° W	5	25	11.3 ± 1.3	55	81.0 ± 5.2	405
15:25	3° N	47° W	3	10	16.7 ± 2.0	56	64.5 ± 5.7	215
15:43	48° S	1° W	54	66	26.7 ± 3.8	33	89.0 ± 9.4	108
16:32	52° N	160° W						

[a]Number does not include star events, which are approximately 35 per compartment.

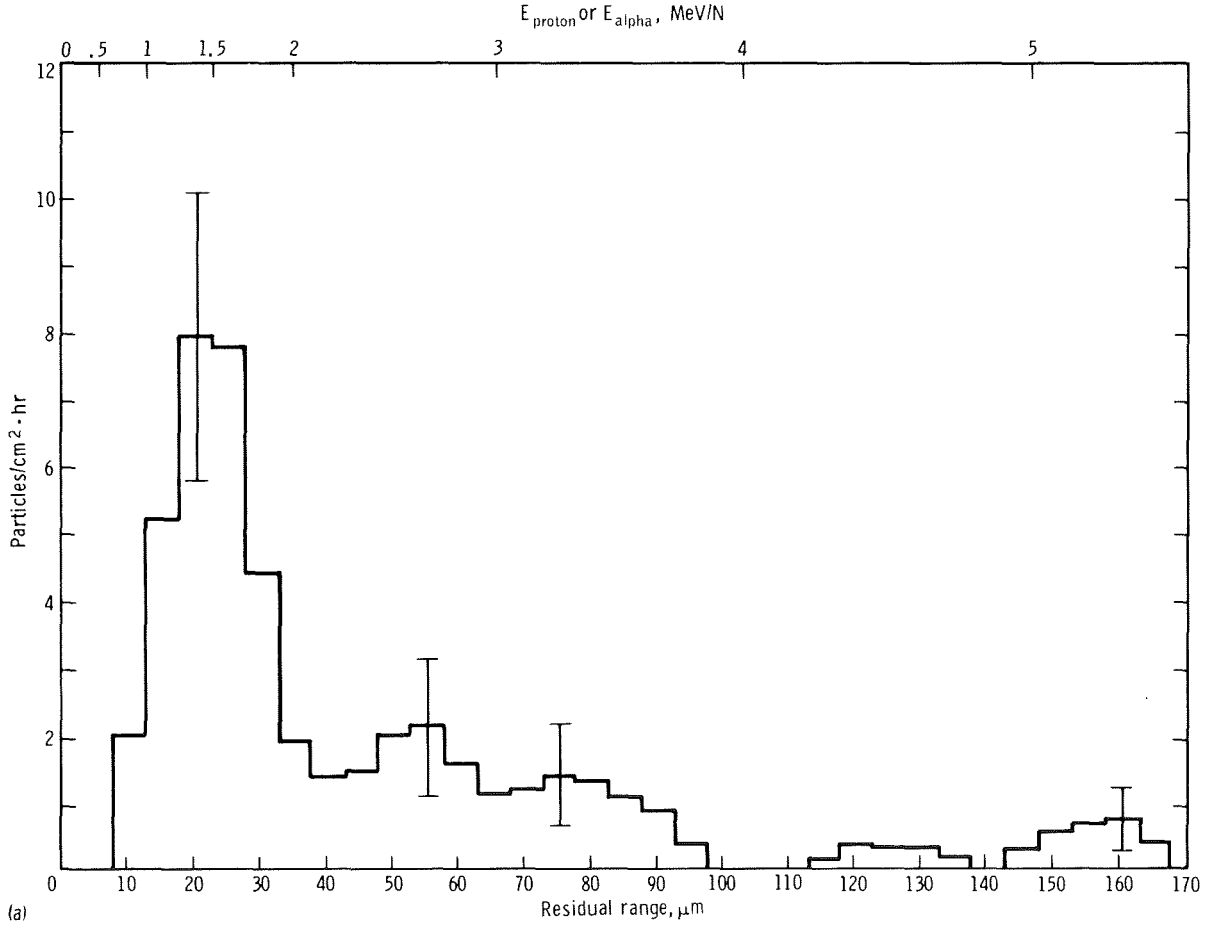

FIGURE 12-7.—Residual range distribution of protons and alpha particles (July 22, 1975). (a) Compartment 1, 14:56 to 15:13 UT. (b) Compartment 2, 15:13 to 15:25 UT. (c) Compartment 3, 15:25 to 15:43 UT. (d) Compartment 4, 15:43 to 16:32 UT.

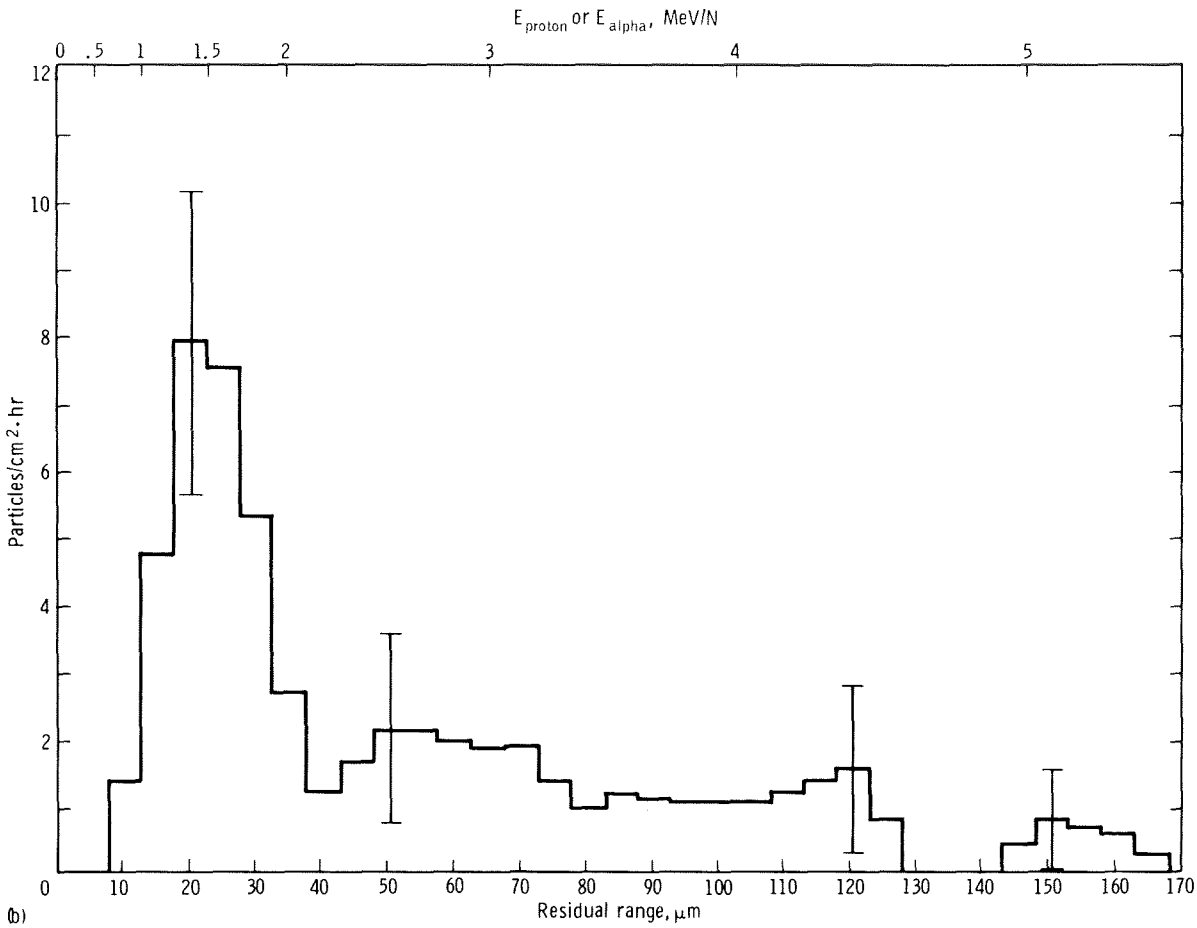

FIGURE 12-7.—Continued.

transited latitudes for varying time intervals, normalization to equal time intervals is shown in figure 12-6(c). A total of 82 events was reported by the two astronauts (table 12-I). No increased activity in the SAA and no graying of the darkened visual fields occurred.

Crystal Detectors

The AgCl(Cd) detectors from the four compartments corresponding to the four sectors of the orbit were analyzed for two categories of events (table 12-II). The first category includes protons and alpha particles that could be seen to enter and stop within the AgCl(Cd) layer equivalent to a tissue thickness of 600 μm. The number of particles was tabulated as a function of residual range for each of the four compartments (fig. 12-7). The second category includes those tracks with an LET greater than 15 keV/μm of tissue, which refers to alpha particles of 5 MeV/amu or less kinetic energy and heavier particles. The flux of stopping alpha particles and protons was corrected for known latency of the crystals and normalized to a unit area of 1 cm^2. The flux of the heavier particles was normalized to 1 cm^2, but no latency correction was used because this correction varies

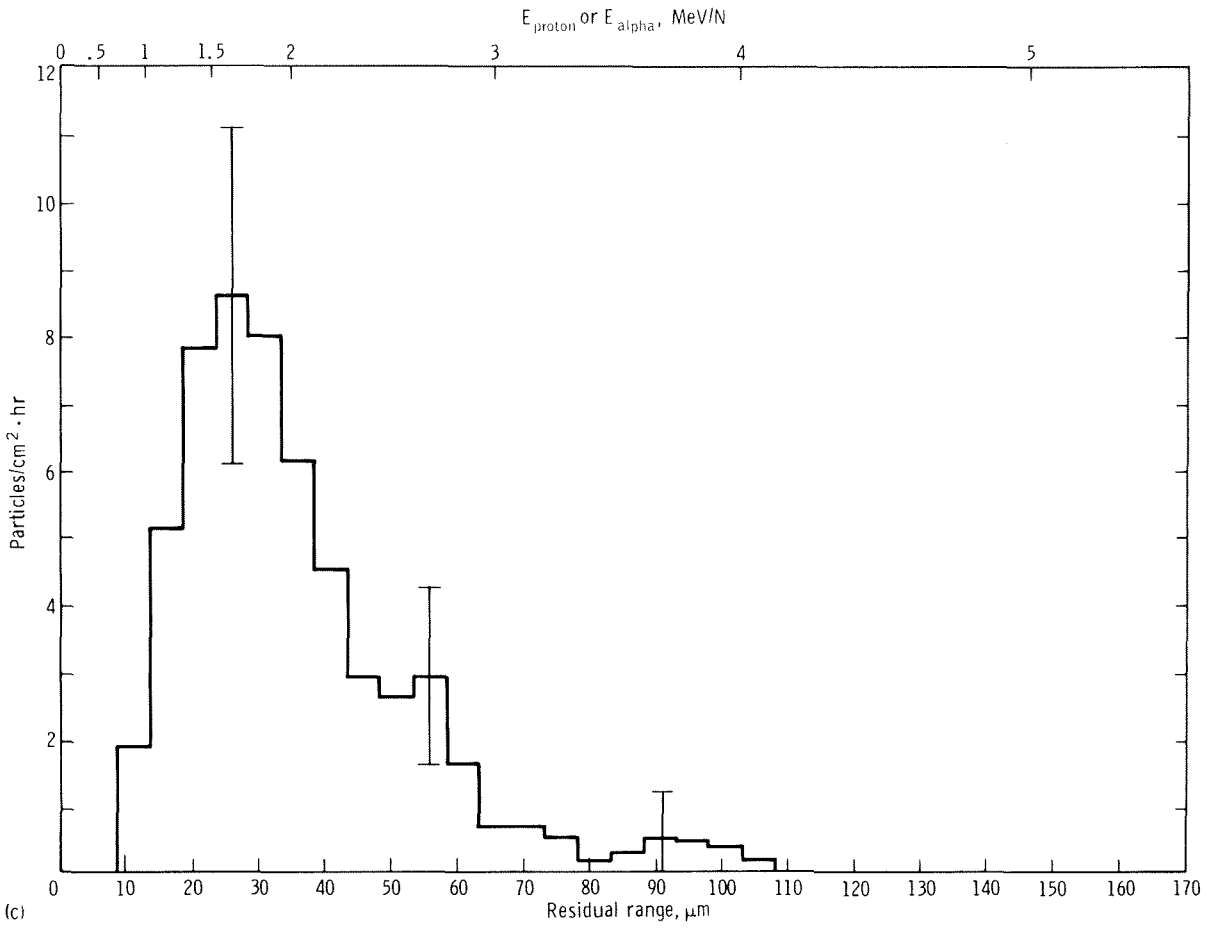

FIGURE 12-7.—Continued.

with the particular ion. Star events were reported in arbitrary units and were of constant abundance in the crystals examined.

The maximum calculated abundances of primary cosmic particles at the north magnetic pole and of trapped protons at the SAA are shown as a function of energy loss in table 12-III. The fluxes are those that are expected at the right-eye position of the right-hand couch in the Apollo spacecraft. The fluxes for 443 km were greater because of less shielding in the observing position during the Skylab 4 mission (ref. 12-6). Distribution of abundances for revolution 111 is shown for various LET ranges in figure 12-8(a). The abundance of trapped protons is shown for LET ranges in figure 12-8(b).

DISCUSSION

Primary Cosmic Particles

The frequency of reported light flash events is strongly dependent on latitude. At the points of closest approach to the geomagnetic poles, the observed events occur at one to two per minute;

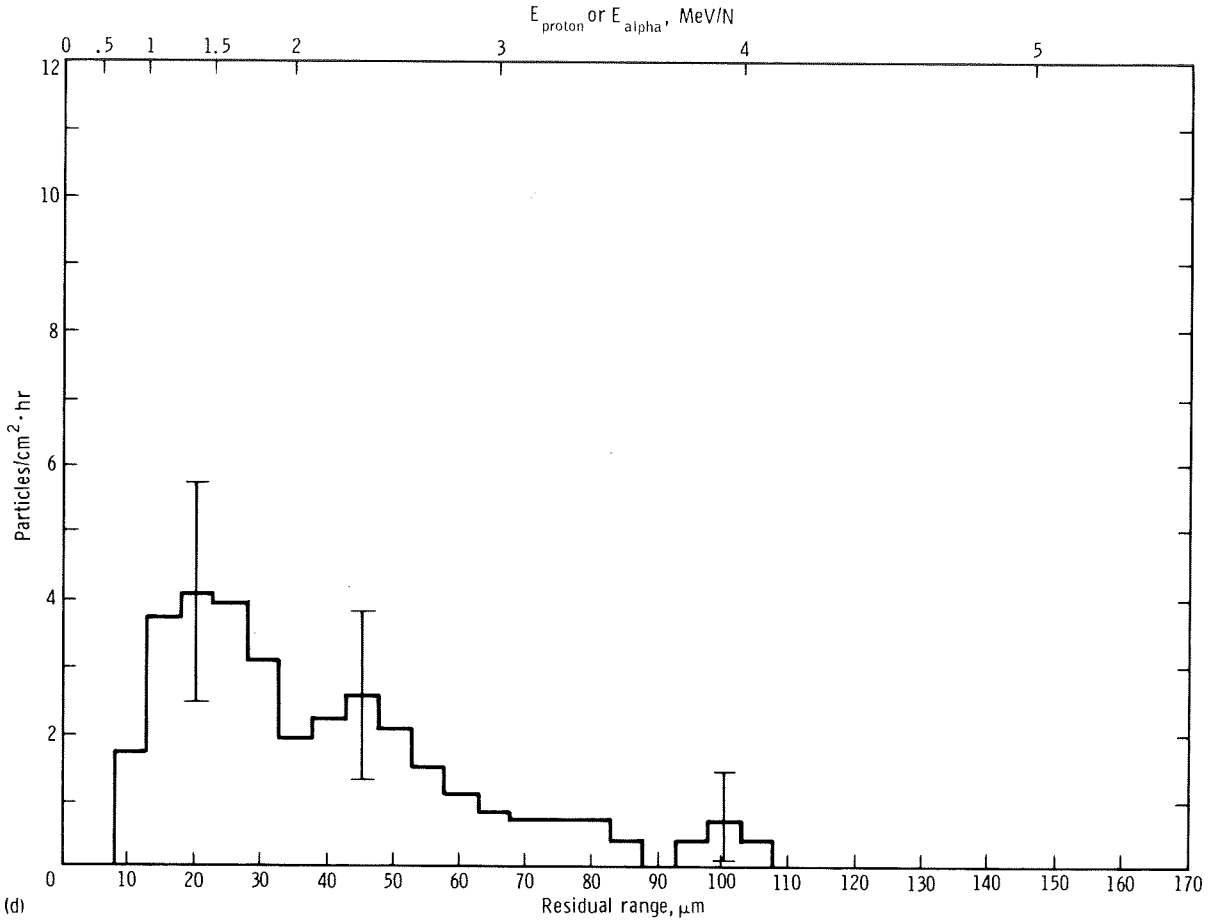

FIGURE 12-7.—Concluded.

TABLE 12-III.—Maximum Abundance of Particles at Right Astronaut Eye

Energy loss, keV/μm	*Protons at SAA, no.*	*Primary cosmic particles at the north magnetic pole*[a] *no./(3 min • 4 cm^2)*		
		Alpha	*$6 \leq Z \leq 9$*	*Cosmic total*
≥0.5	114 200	117	10	135
≥1	5 813	51	10	67
≥5	241	.4	6	10
≥10	53	.07	3	6
≥15	22	.03	2	4
[b]≥15	[b]318	[b].08	[b]2	[b]4
≥20	11	.02	1	3
≥25	7	.01	.5	2

[a]South magnetic pole maximum abundances are 8 percent less.
[b]For 443-km altitude of Skylab 4 but shielding of Apollo.

however, no events were observed near the Equator (fig. 12-6(c)). These observations are consistent with the change in abundance of cosmic particles with latitude (figs. 12-6 and 12-8(a)), which was also noted during the Skylab 4 mission (ref. 12-6). The increased rate of visual events near the south geomagnetic pole can be explained by the increased dark adaptation of the crewmembers. The observed event rate correlates with a cosmic particle abundance for heavy particles with energy losses $\geq$5 keV/μm (fig. 12-8(a)). The previous experiments indicate that the threshold for high-efficiency visualization of primary events is 10 keV/μm (refs. 12-13 and 12-15), but the calculated flux for ions of 10 keV/μm and greater is too low to correspond to the observed rate (table 12-III and fig. 12-8(a)). This discrepancy could be resolved by increasing the abundances by a factor of 2, which might be appropriate because the calculations did not include the change in the modulation of the cosmic spectrum associated with the solar cycle.

The AgCl(Cd) detector results (table 12-II) suggest that 60 events of 15 keV/μm or greater would be observed during 3-minute intervals in the northernmost portions of the orbit. The highest observed event rate at high latitudes was only 14 events/3 min near the south magnetic pole. This rate would imply a 23-percent efficiency; however, near the Equator, where only a few events were observed, the detectors recorded the equivalent average of 73 events/4 cm^2 · min.

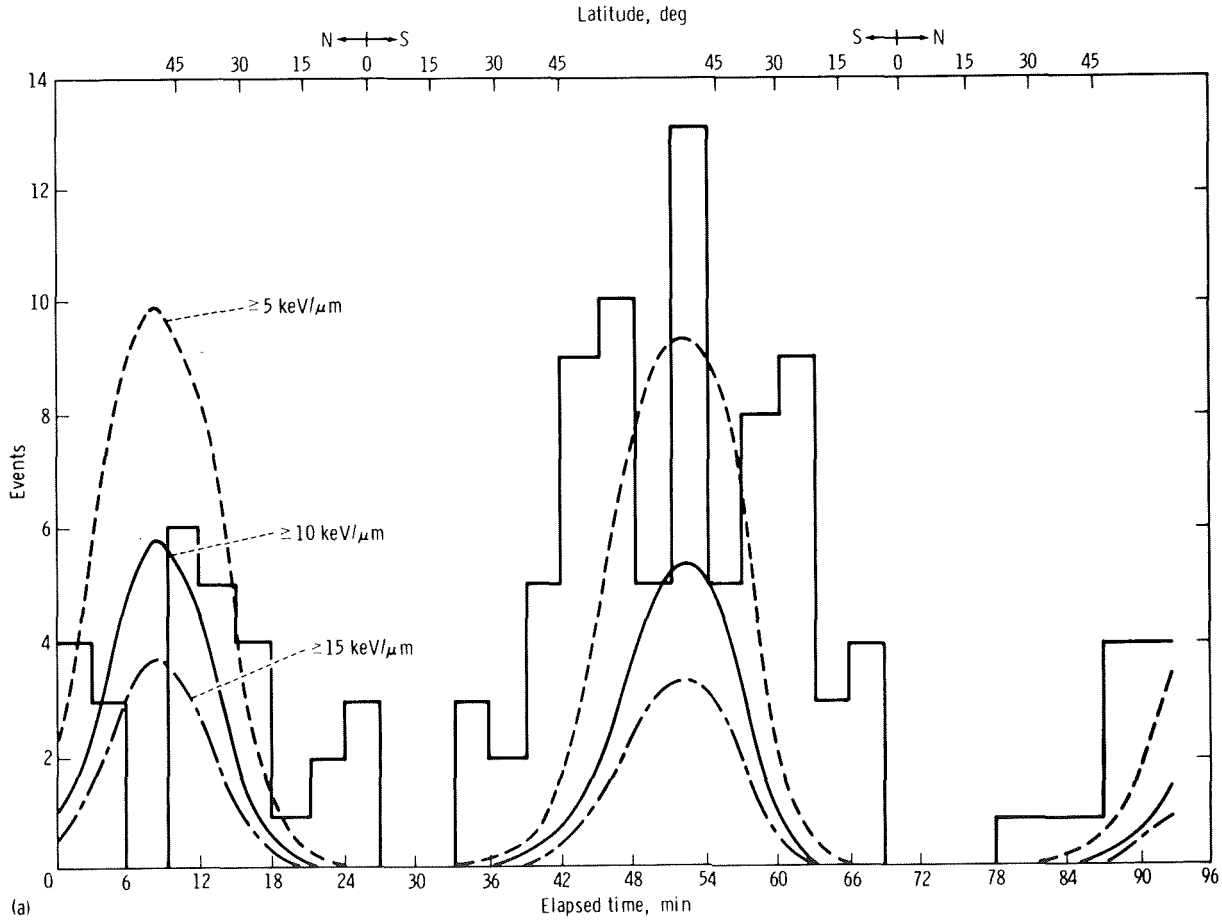

FIGURE 12-8.—Comparison of calculated abundances (curves) to observed events (histograms). (a) Cosmic particles. (b) Trapped protons.

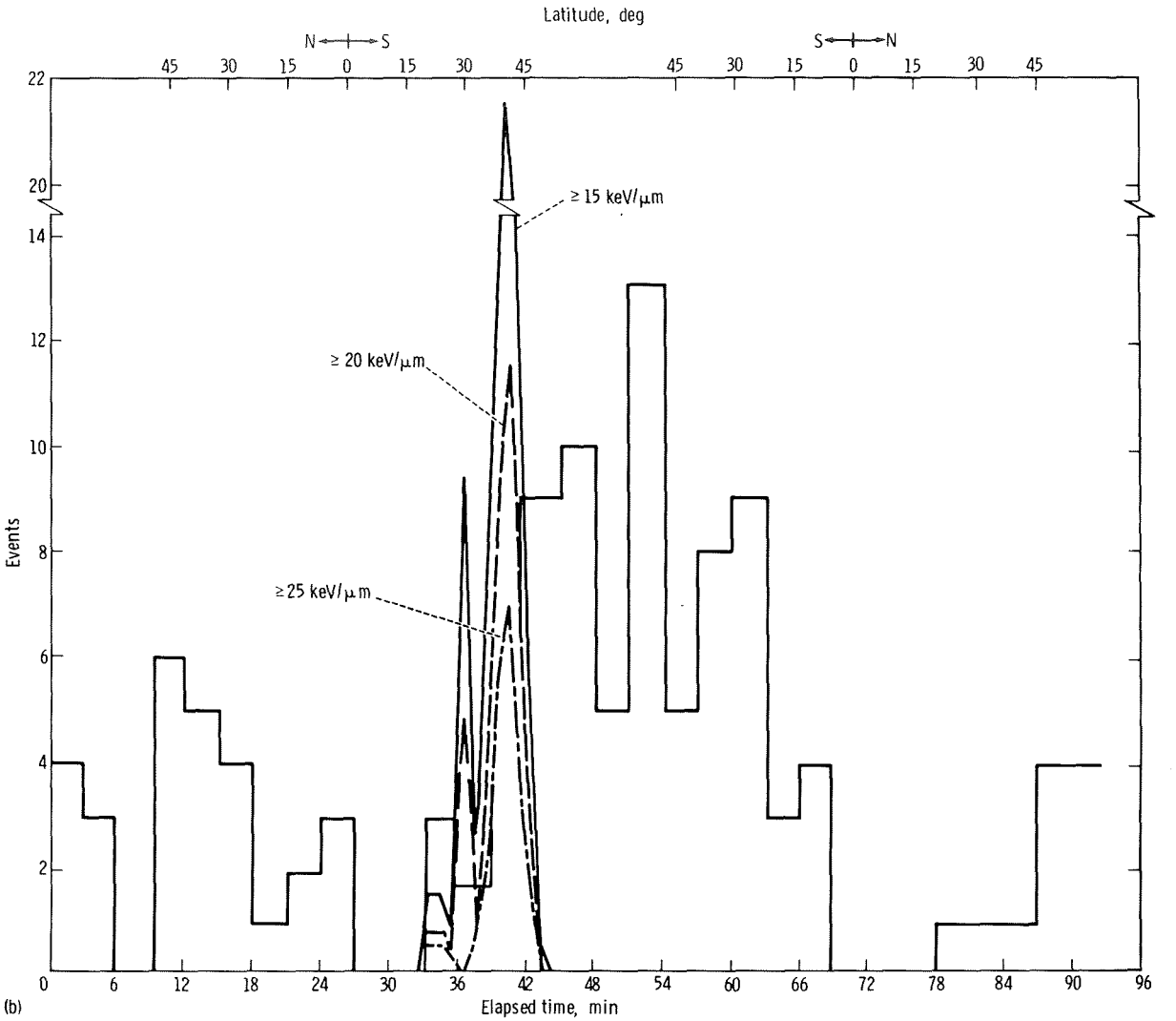

FIGURE 12-8.—Concluded.

These results are not consistent. An explanation is that the fading time from the heavy ions is long relative to the orbit sectors; thus, good identification of the very heavy particle environment in each sector cannot be expected. Particles interacting in the crystals hours before the experiment might have been included in the count.

Better time discrimination is expected from the stopping protons and alpha particles (table 12-II). Assuming the complete retina target area is 4 cm^2, the efficiency of visualizing these events is 36 percent for the northernmost sector; but here also, the efficiency diminishes to only 8 percent for the SAA. Thus, the AgCl(Cd) detector data do not correlate well with either the observed event rate or the calculated abundances.

South Atlantic Anomaly Observations

There were no reports of a high frequency of flash phenomena through the SAA, as might be expected from a previous Skylab 4 report of markedly increased flash activity (ref. 12-6). Only

four events were reported in this region for Apollo-Soyuz (fig. 12-5), whereas 112 events were reported in a 12-minute period through the SAA during Skylab 4. At the 225-km altitude of Apollo-Soyuz, the proton flux of particles (LET $\geq$15 keV/μm) is 14 times less than at the 443-km altitude of Skylab 4. Also, the shielding of the Apollo command module is much greater than that of Skylab. The Apollo command module shielding was 3.0 to 3.5 g/cm^2 of aluminum over a solid angle of 0.27π sr and 3.5 to 5.5 g/cm^2 over 0.77π-sr solid angle, whereas the observations from Skylab were made in a minimum shielding area of 1.5 to 2.0 g/cm^2 over 1.5π sr.

The distribution of protons near the astronauts' eyes along the orbit is shown in figure 12-8(b). Although the abundance of protons with energy loss $\geq$15 keV/μm is great enough to explain the few events seen in the SAA region at latitude 35° S (fig. 12-6(b)), a group of events that correspond to

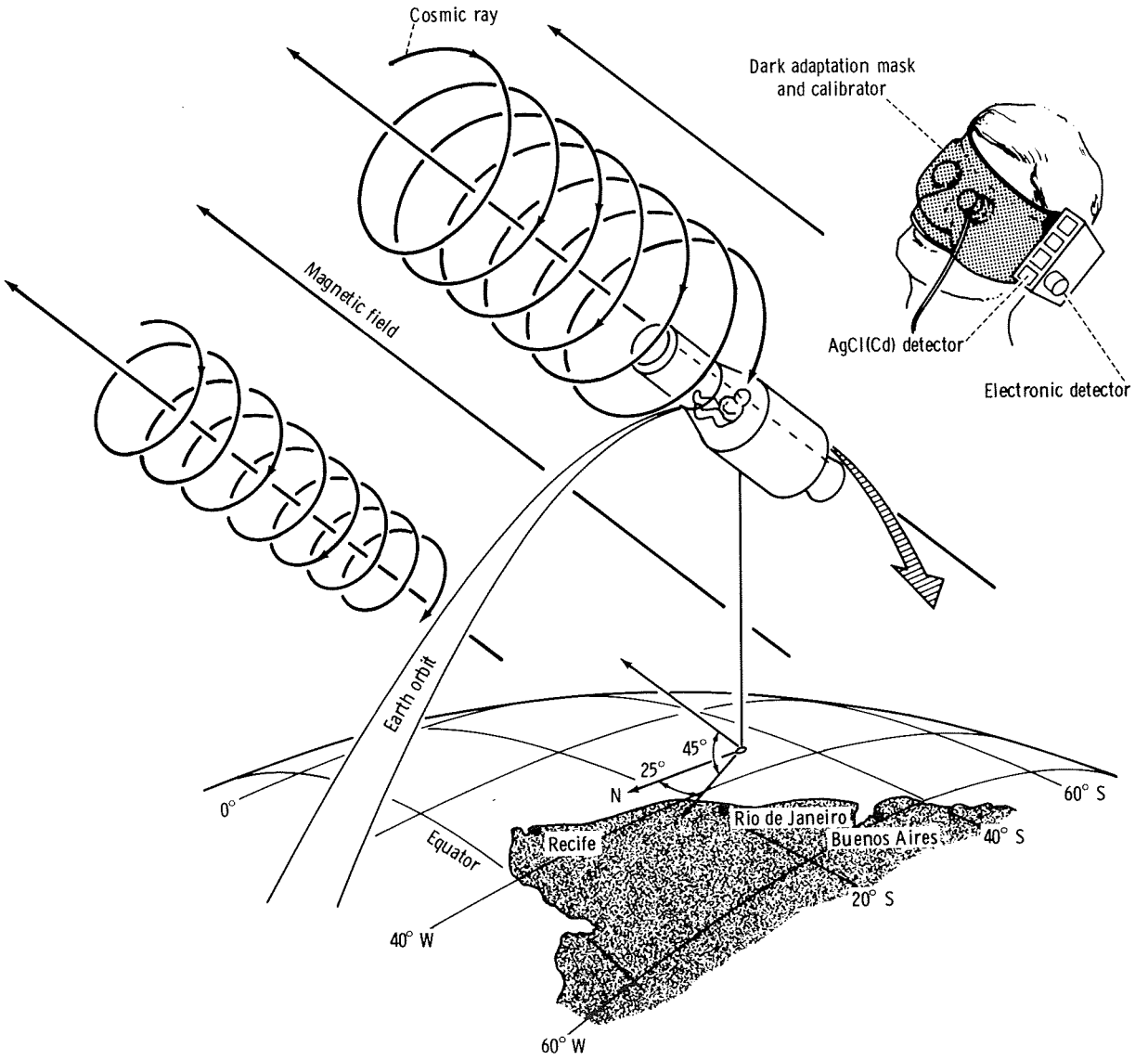

FIGURE 12-9.—Orientation of the spacecraft and astronauts during passage over the SAA.

the SAA cannot be statistically separated. Care was taken to orient the spacecraft and crewmembers so that the particle trajectories would cross the posterior eye orbit tangentially (fig. 12-9). From accelerator experiments, as well as a consideration of maximum path length in the retina, this orientation optimizes the efficiency of the human eye and the AgCl(Cd) crystal detectors. The hypothesis that protons with an LET of $\geq$15 keV/μm cause these observed streaks is questionable because these protons have a range of only 100 μm and could not cause a streak because they would intersect 10 retinal rods or less.

An alternate explanation for events seen in the SAA, particularly at higher altitudes, is the mechanism of proton nonelastic nuclear collision with carbon, hydrogen, and oxygen in tissues of the retina. This mechanism is similar to that proposed for neutron interactions, which also cause discrete flashes (refs. 12-12 and 12-13). If the average cross section for interactions such as $(p, p', 3\alpha)$ on carbon, nitrogen, or oxygen is assumed to be approximately 45 fm^2 (450 mb) in the proton energy range of 175 MeV or less, only 1 event/3 min would occur during Apollo-Soyuz; however, at the Skylab 4 altitude, the flux of protons was 23 times greater than at the Apollo-Soyuz altitude of 225 km (table 12-III). Under the reduced shielding conditions of Skylab 4, 51 times more protons would interact with the eye tissues of one observer, or 26 events might be observed during a 3-minute interval. The average rate was 28 events/3 min. Thus, the nuclear collision hypothesis for the origin of light flashes in the SAA has some validity.

ACKNOWLEDGMENTS

The following persons made important contributions to this project: W. Greenberg, University of California at Berkeley; J. Kucala, Lawrence Livermore Laboratory; and R. Dowling, F. Goulding, B. Moyer, J. Walton, and R. Walton, Lawrence Berkeley Laboratory.

REFERENCES

12-1. Chapman, P. K.; Pinsky, L. S.; Benson, R.E.; and Budinger, T. F.: Observations of Cosmic Ray Induced Phosphenes. Proceedings of the National Symposium on Natural and Manmade Radiation in Space, E. A. Warren, ed. NASA TM X-2440, 1972, pp. 1002-1006.

12-2. Budinger, T. F.; Tobias, C. A.; et al.: Light Flash Phenomenon Seen by Astronauts. Proceedings of the Colloquium on Space Biology Related to Post-Apollo Program. ESRO, Paris, France, 1971, p. 209.

12-3. Benson, R. E.; and Pinsky, L. S.: Visual Light Flash Phenomenon. Sec. 27, Pt. C, of the Apollo 16 Preliminary Science Report. NASA SP-315, 1972.

12-4. Pinsky, L. S.; Osborne, W. Z.; and Bailey, J. V.: Visual Light Flash Phenomenon. Sec. 27 of the Apollo 17 Preliminary Science Report. NASA SP-330, 1973.

12-5. Pinsky, L. S.; Osborne, W. Z.; et al.: Light Flashes Observed by Astronauts on Apollo 11 Through Apollo 17. Science, vol. 183, no. 4120, Mar. 8, 1974, pp. 957-959.

12-6. Pinsky, L. S.; Osborne, W. Z.; Bailey, J. V.; and Hoffman, R. A.: Light Flashes Observed by Astronauts on Skylab 4. Science, vol. 188, no. 4191, May 30, 1975, pp. 928-930.

12-7. Tobias, C. A.: Radiation Hazards in High Altitude Aviation. J. Aviation Med., vol. 23, 1952, p. 345.

12-8. Fazio, G. G.; Jelley, J. V.; and Charman, W. N.: Generation of Cerenkov Light Flashes by Cosmic Radiation Within the Eyes of the Apollo Astronauts. Nature, vol. 228, no. 5268, Oct. 17, 1970, pp. 260-264.

12-9. McNulty, P. J.: Light Flashes Produced in the Human Eye by Extremely Relativistic Means, Nature, vol. 234, no. 5323, Nov. 12, 1971, p. 110.

12-10. McNulty, P. J.; Pease, V. P.; et al.: Visual Sensations Induced by Relativistic Nitrogen Nuclei. Science, vol. 178, no. 4056, Oct. 13, 1972, p. 160.

12-11. McNulty, P. J.; Pease, V. P.; and Bond, V. P.: Visual Sensations Induced by Cerenkov Radiation. Science, vol. 189, no. 4201, Aug. 8, 1975, pp. 453-454.

12-12. Tobias, C. A.; Budinger, T. F.; and Lyman, J. T.: Radiation-Induced Light Flashes Observed by Human Subjects in Fast Neutron, X-ray, and Positive Pion Beams. Nature, vol. 230, Apr. 30, 1971, pp. 596-597.

12-13. Budinger, T. F.; Bichsel, H.; and Tobias, C. A.: Visual Phenomena Noted by Human Subjects on Exposure to Neutrons of Energies Less Than 25 Million Electron Volts. Science, vol. 172, no. 3978, May 21, 1971, pp. 868-870.

12-14. Tobias, C. A.; Budinger, T. F.; and Lyman, J. T.: Biological Effects Due to Single Accelerated Heavy Particles - Problems of Nervous System Exposure in Space. In Life Sciences and Space Research XI, P. H. A. Sneath, ed., Academie-Verlag (Berlin), 1973, p. 233.

12-15. Budinger, T. F.; Lyman, J. T.; and Tobias, C. A.: Visual Perception of Accelerated Nitrogen Nuclei Interacting With the Human Retina. Nature, vol. 239, no. 5369, Sept. 22, 1972, pp. 209-211.

12-16. Schott, J.-U.: Eigenshaften von AgCl(Cd)-Kristallen als Teilchenspur-Detektoren. Ph. D. Thesis, Institut für Kernphysik der Johann Wolfgang Goethe-Universität Frankfurt Am Main, 1974.

12-17. Webber, W. R.; Damle, S. V.; and Kish, J.: Studies of the Chemical Composition of Cosmic Rays with Z = 3-30 at High and Low Energies. Astrophys. Space Sci., vol. 15, Feb. 1972, pp. 245-271.

12-18. Smith, L. H.; Buffington, A.; et al.: A Measurement of Cosmic-Ray Rigidity Spectra Above 5 GV/c of Elements From Hydrogen to Iron. Astrophys. J., vol. 180, no. 3, Mar. 1973, pp. 987-1010.

12-19. Juliusson, E.: Cosmic Rays at Very High Energies. Vol. I, Proceedings of the 13th International Cosmic Ray Conference, 1974, pp. 373-377.

12-20. Lavine, J. P.; and Vette, J. I.: Models of the Trapped Radiation Environment. Vol. VI - High Energy Protons. NASA SP-3024, 1970.

12-21. Hendricks, S. J.; and Cain, J. C.: Magnetic Field Data for Trapped-Particle Evaluations. J. Geophys. Res., vol. 71, no. 1, Jan. 1, 1966, pp. 346-349.

12-22. Shea, M. A.; and Smart, D. F.: A Five by Fifteen Degree World Grid of Calculated Cosmic-Ray Vertical Cutoff Rigidities for 1965 and 1975. Vol. 4, Proceedings of the 14th International Cosmic Ray Conference, 1975, pp. 1298-1304.

12-23. Smart, D. F.; and Shea, M. A.: A Study of the Effectiveness of the McIlwain Coordinates in Estimating Cosmic-Ray Vertical Cutoff Rigidities. J. Geophys. Res., vol. 72, no. 13, July 1, 1967, pp. 3447-3454.

12-24. Smart, D. F.; and Shea, M. A.: An Analysis of Trajectory-Derived Penumbral Widths. Vol. 4, Proceedings of the 14th International Cosmic Ray Conference, 1975, pp. 1309-1314.